The Intramolecular Force Field and Normal Vibrations of Isotactic Polypropylene and Deuterated Derivatives[*1]

By Tatsuo MIYAZAWA and Yoshiko IDEGUCHI

(Received February 24, 1964)

The infrared active normal vibrations of isotactic polypropylene (IPP), poly(propylene-2-d_1) (IPP-CD), poly(propylene-1, 1-d_2) (IPP-CD_2) and poly(propylene-3, 3, 3-d_3) (IPP-CD_3) in the 1500~650 cm^{-1} region have been treated in previous studies.[1,2] The high-frequency CH stretching modes of the CH, CH_2, and CH_3 groups have been separated and the internal rotation modes have not been taken into account since the internal rotation potential terms do not contribute much to the frequencies above 650 cm^{-1}. Thus, the "effective" potential constants have been calculated, by the method of least squares,[3] from the observed frequencies. In the present study, a complete normal coordinate treatment of isotactic polypropylene and deuterated derivatives was made, one in which the CH stretching modes and the internal-rotation modes about the CH–CH_2 and CH–CH_3 bonds were all taken into account.

Normal Coordinate Treatment

Internal Coordinates.—A general method for the treatment of the molecular vibrations of helical polymers has been described.[1] The internal coordinate (or the local symmetry coordinate) vectors, $R_{1,n}$~$R_{18,n}$, of the nth repeating unit of isotactic polypropylene have been given in Eqs. 1—6 of Ref. 2. In addition, the C–H stretching coordinates and the internal rotation coordinaten shown below were used in the present study:

$$R_{19,n}(\text{CH stretch.}) = \Delta r(1,n;\ 5,n) \tag{1}$$

$$\begin{bmatrix} R_{20,n}(\text{CH}_3 \text{ sym. stretch.}) \\ R_{21,n}(\text{CH}_3 \text{ asym. stretch.}) \\ R_{22,n}(\text{CH}_3 \text{ asym. stretch.}) \end{bmatrix} = \begin{bmatrix} 1/3^{1/2} & 1/3^{1/2} & 1/3^{1/2} \\ 1/6^{1/2} & 1/6^{1/2} & -2/6^{1/2} \\ 1/2^{1/2} & -1/2^{1/2} & 0 \end{bmatrix} r(\text{CH}_3)_n \tag{2}$$

$$\begin{bmatrix} R_{23,n}(\text{CH}_2 \text{ sym. stretch.}) \\ R_{24,n}(\text{CH}_2 \text{ asym. stretch.}) \end{bmatrix} = \begin{bmatrix} 1/2^{1/2} & 1/2^{1/2} \\ 1/2^{1/2} & -1/2^{1/2} \end{bmatrix} r(\text{CH}_2)_n \tag{3}$$

where the elements of the vector $r(CH_3)$ in Eq. 2 are $\Delta r(3,n;\ 7,n)$, $\Delta r(3,n;\ 8,n)$, and $\Delta r(3,n;\ 9,n)$; the elements of the vector r-$(CH_2)_n$ in Eq. 3 are $\Delta r(2,n;\ 4,n)$ and $\Delta r(2,n;\ 6,n)$; and Δr's are the stretching coordinates for which the numbering of carbon and hydrogen atoms has been shown in Fig. 1 of Ref. 2.

The internal-rotation coordinates[4] for the nth unit are;

$$\begin{aligned} R_{25,n}(\text{CH–CH}_3 \text{ bond}) &= \Delta t(1,n;\ 3,n) \\ &= [\Delta\tau(2,n-1;\ 1,n;\ 3,n;\ 7,n) \\ &\quad + \Delta\tau(2,n-1;\ 1,n;\ 3,n;\ 8,n) \\ &\quad + \Delta\tau(2,n-1;\ 1,n;\ 3,n;\ 9,n) \\ &\quad + \Delta\tau(2,n;\ 1,n;\ 3,n;\ 7,n) \\ &\quad + \Delta\tau(2,n;\ 1,n;\ 3,n;\ 8,n) \\ &\quad + \Delta\tau(2,n;\ 1,n;\ 3,n;\ 9,n) \\ &\quad + \Delta\tau(5,n;\ 1,n;\ 3,n;\ 7,n) \\ &\quad + \Delta\tau(5,n;\ 1,n;\ 3,n;\ 8,n) \\ &\quad + \Delta\tau(5,n;\ 1,n;\ 3,n;\ 9,n)]/9 \end{aligned} \tag{4}$$

$$\begin{aligned} R_{26,n}(\text{axial CH–CH}_2 \text{ bond}) &= \Delta t(1,n;\ 2,n) \\ &= [\Delta\tau(2,n-1;\ 1,n;\ 2,n;\ 4,n) \\ &\quad + \Delta\tau(2,n-1;\ 1,n;\ 2,n;\ 6,n) \\ &\quad + \Delta\tau(2,n-1;\ 1,n;\ 2,n;\ 1,n+1) \\ &\quad + \Delta\tau(3,n;\ 1,n;\ 2,n;\ 4,n) \\ &\quad + \Delta\tau(3,n;\ 1,n;\ 2,n;\ 6,n) \\ &\quad + \Delta\tau(3,n;\ 1,n;\ 2,n;\ 1,n+1) \\ &\quad + \Delta\tau(5,n;\ 1,n;\ 2,n;\ 4,n) \\ &\quad + \Delta\tau(5,n;\ 1,n;\ 2,n;\ 6,n) \\ &\quad + \Delta\tau(5,n;\ 1,n;\ 2,n;\ 1,n+1)]/9 \end{aligned} \tag{5}$$

$$\begin{aligned} R_{27,n}(\text{equatorial CH–CH}_2 \text{ bond}) &= \Delta t(2,n;\ 1,\ n+1) \\ &= [\Delta\tau(1,n;\ 2,n;\ 1,n+1;\ 2,n+1) \\ &\quad + \Delta\tau(1,n;\ 2,n;\ 1,n+1;\ 3,n+1) \\ &\quad + \Delta\tau(1,n;\ 2,n;\ 1,n+1;\ 5,n+1) \\ &\quad + \Delta\tau(4,n;\ 2,n;\ 1,n+1;\ 2,n+1) \end{aligned}$$

*1 This is Part VI of *Molecular Vibrations and Structures of High Polymers*. The present study was, in part, published at the Confernce on Vibrational Spectra of High Polymers, Milan, July, 1963.

1) T. Miyazawa, Y. Ideguchi and K. Fukushima, *J. Chem. Phys.*, **38**, 2709 (1963).
2) T. Miyazawa and Y. Ideguchi, This Bulletin, **36**, 1125 (1963).
3) D. E. Mann, T. Shimanouchi, J. H. Meal and L. Fano, *J. Chem. Phys.*, **27**, 43 (1957).

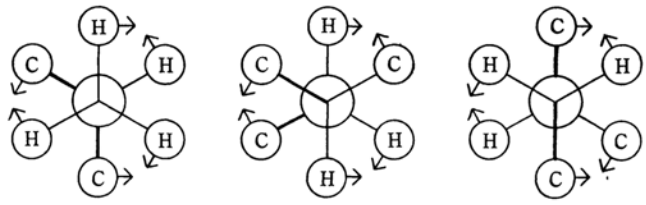

Fig. 1 The internal-rotation modes about the C-methyl bond (t_{C-CH_3}), about the axial C-C bond (t_{CC}^{ax}), and about the equatorial C-C bond (t_{CC}^{eq}) of isotactic polypropylene chain (the right-handed helix). Main chain C-C bonds are drawn with heavy lines.

$$+\Delta\tau(4,n;\ 2,n;\ 1,n+1;\ 3,n+1)$$
$$+\Delta\tau(4,n;\ 2,n;\ 1,n+1;\ 5,n+1)$$
$$+\Delta\tau(6,n;\ 2,n;\ 1,n+1;\ 2,n+1)$$
$$+\Delta\tau(6,n;\ 2,n;\ 1,n+1;\ 3,n+1)$$
$$+\Delta\tau(6,n;\ 2,n;\ 1,n+1;\ 5,n+1)]/9 \qquad (6)$$

where $\Delta\tau$'s are the torsional coordinates. These internal-rotation coordinates are schematically shown in Fig. 1. The elements of the inverse kinetic energy matrix associated with the internal-rotation modes were calculated by the use of the general formulas.[4]

Potential Function.—In deriving the potential energy matrix, the modified Urey-Bradley field was supplemented with these internal-rotation potential term.[4,5]

$$V(\text{internal-rotation}) = \frac{1}{2}\sum_n \{Y(\text{CH–CH}_2)\,[\Delta t(1,n;\ 2,n)]^2 + Y(\text{CH–CH}_2)\,[\Delta t(2,n;\ 1,n+1)]^2 + Y(\text{CH–CH}_3)\,[\Delta t(1,n;\ 3,n)]^2\} \qquad (7)$$

The potential constants of isotactic polypropylene used in the present study are listed in Table I. Common potential constants, K(C–C) and Y(C–C), were used for the axial and equatorial CH–CH$_2$ bonds, since the arrangements of the carbon and hydrogen atoms adjacent to these C–C bonds are the same. The repulsion constants, F(H–C–H) and F(C–C–H), were transferred from the ethane molecule as treated by Takahashi and Shimanouchi.[6] The initial set of the remaining potential constants (except for the CH stretching constant) were transferred from the previous study[2] and were then adjusted by the method of least squares[3] with reference to the fundamental frequencies of IPP, IPP-CD, IPP-CD$_2$, and IPP-CD$_3$ as observed by Peraldo and Farina[7] in the region above 650 cm^{-1} and to the far infrared frequencies of IPP in the region below 650 cm^{-1}.[1,8] The adjustments of the potential constants were repeated until

Table I. Modified Urey-Bradley potential constants*1 (and standard error*2) of isotactic polypropylene

K(C-H)	4.255±0.003	CH_3 group
	3.980±0.005	CH_2 group
	4.030±0.003	CH group
K(C-C)	2.240±0.108	CH-CH_2 bond
	2.270±0.110	CH-CH_3 bond
Y(C-C)	0.176±0.042	CH-CH_2 bond
	0.080±0.002	CH-CH_3 bond
H(H-C-H)	0.366±0.002	CH_3 group
	0.353±0.004	CH_2 group
H(H-C-C)	0.231±0.011	CH_3 group
	0.218±0.006	CH_2 group
	0.235±0.016	CH group
H(C-C-C)	0.350±0.100	C-CH_2-C angle
	0.390±0.035	C-CH-C angle
F(H-C-H)	0.200*3	
F(H-C-C)	0.480*3	
F(C-C-C)	0.280±0.065	
κ	−0.028±0.008	CH_3 group
	0.002±0.012	CH_2 group
	−0.130±0.055	CH group
T	0.118±0.007	H-C-C-H (trans)
G	−0.038±0.007	H-C-C-H (gauche)
p(C-H)	−0.115±0.005	CH_3 group
	−0.115±0.015	CH_2 group
l(C-C-H)	0.000±0.005	C-CH_2-C

*1 K, stretching (mdyn./Å); Y, internal rotation (mdyn.Å); H, bending (mdyn./Å;) F, repulsion (mdyn./Å); T, trans-coupling (mdyn.Å); G, gauche-coupling (mdyn.Å); κ, intramolecular tension (mdyn.Å), l, angle-interaction (mdyn. Å), and p, stretching-interaction (mdyn./Å).
*2 Ref. 10.
*3 Transferred from ethane (Ref. 6).

4) T. Miyazawa and K. Fukushima, 16th Annual Meeting of the Chemical Society of Japan, Tokyo, April, 1963.
5) T. Shimanouchi, *Pure Appl. Chem.*, **7**, 131 (1963).
6) H. Takahashi and T. Shimanouchi, Symposium on Molecular Structure, Sendai, October (1963).
7) M. Peraldo and M. Farina, *Chim. Ind. (Milan)*, **42**, 1349 (1960).
8) T. Miyazawa, K. Fukushima and Y. Ideguchi, *J. Polymer Sci.* **B1**, 385 (1963).

finally, for each constant, the calculated correction was reduced to a point where it was negligible compared with the standard error. In the adjustment of the potential constant, the element of the Jacobian matrices were calculated by the equation reported previously.[9] The standard errors were calculated according to the method derived by Ogawa and Miyazawa.[10]

Potential Constants. — The final set of the potential constants and their standard errors are listed in Table I. The C–H stretching constants, K(C–H), of the CH_2 and CH groups are calculated to be slightly smaller than for the CH_3 group, where the repulsion constants, F(H–C–H) and F(C–C–H), have been transferred from ethane. The stretching-interaction constants, p(C–H), for the CH_3 and CH_2 groups were taken independently, but they have finally been calculated to be the same. Therefore, a common stretching-interaction parameter may be used for the CH_3 and CH_2 groups.

The stretching constants, K(C–C), for the CH–CH_2 and CH–CH_3 bonds were also taken independently, but these two constants finally coincided within the standard errors. Therefore, these two constants may well be reduced to a common parameter $[(2.240+2.270)/2 = 2.255]$.

The bending constants of the H–C–H angle of the CH_3 and CH_2 groups are nearly the same, but the difference is greater than their standard errors. The bending constants for the C–C–H angles of the CH_3, CH_2, and CH groups all lie in the range between 0.235 and 0.215 mdyn./Å.

The values of the intramolecular tension [κ] and angle-interaction term [l(C–C–H)]*2 for the CH_2 group are almost negligible compared with the corresponding standard errors; accordingly, these parameters may well be neglected, at least in the treatment of polypropylene. It may be recalled that the corresponding contants for malonitrile, $CH_2(CN)_2$, are also negligible.[5]

The trans and gauche coupling constants of IPP agree closely with those of ethane ($T=0.107$ and $G=-0.024$) and of polyethylene ($T=0.100$ and $G=-0.033$).[5]

The internal-rotation constants, Y(C–C), may be used for estimating the barrier height of the internal-rotation potential, which is assumed to be threefold and sinusoidal. Thus, the potential barrier for the CH–CH_2 bond of the main chain and for the CH–CH_3 bond are estimated to be 5.7 ± 1.4 and 2.9 ± 0.1 kcal./mol. (approximately corrected for anharmonicity[4]) respectively.

The diagonal elements of the potential energy matrix associated with genuine vibrational modes may be obtained satisfactorily from the observed frequencies, although the off diagonal elements are not necessarily so.[5] Accordingly, the final values of the diagonal elements associated with "local" symmetry coordinates of isotactic polypropylene are listed in Table II.

Table II. The diagonal elements*1 of the potential energy matrix of isotactic polypropylene

CH_3 sym. stretch. (R_{20})	4.798
asym. stretch. (R_{21}, R_{22})	4.726
CH_2 sym. stretch. (R_{23})	4.614
antisym. stretch. (R_{24})	4.566
CH stretch. (R_{19})	4.756
CH–CH_2 stretch. (R_{12}, R_{18})	3.854
CH–CH_3 stretch. (R_6)	4.067
CH_3 sym. deform. (R_9)	0.584
asym. deform. (R_7, R_8)	0.519
rock. (R_{10}, R_{11})	0.686
CH_2 bend. (R_{14})	0.547
wag. (R_{15})	0.677
twist. (R_{16})	0.675
rock. (R_{17})	0.677
CH bend. (R_1, R_2)	0.657
C–CH_2–C bend. (R_{13})	1.021
C–CH$\langle$C sym. deform. (R_3)	0.810
C asym. deform. (R_4, R_5)	1.145
CH–CH_2 internal rotation (R_{26}, R_{27})	0.176
CH–CH_3 internal rotation (R_{25})	0.080

*1 The elements associated with the stretching modes are given in unit of mdyn./Å and the elements associated with the bending and internal rotation coordinates are given in unit of mdyn.Å.

The A and E($2\pi/3$) frequencies of IPP, IPP-CD, IPP-CD_2, and IPP-CD_3 were calculated with the final set of potential constants and are listed in Tables III—IX, together with the observed frequencies. The calculated and observed frequencies are also compared in Figs. 2 and 3. For the region above 650 cm^{-1}, the r.m.s. frequency deviations are: IPP: 0.9%; IPP-CD: 0.9%; IPP-CD_2: 0.8%; and IPP-CD_3: 1.0%; while the overall r.m.s. deviation was 0.9%. Since the calculated frequencies agreed so closely with the observed frequencies, the potential energy distributions were also calculated as aids in assigning the infrared bands. The distributions, $(PED)_{ii}$,

9) T. Miyazawa, *J. Chem. Soc. Japan, Pure Chem. Sec.* (*Nippon Kagaku Zassi*), **76**, 1132 (1955).

10) T. Ogawa and T. Miyazawa, *Spectrochim. Acta*, **20**, 557 (1964).

*2 The parameter, l(C-C-H), is correlated somewhat with the internal-rotation constant for the CH–CH_2 bond. In our previous treatment, the internal-rotation potential terms were neglected and the value of l(C-C-H) was adjusted to 0.014 mdyn./Å.[2]

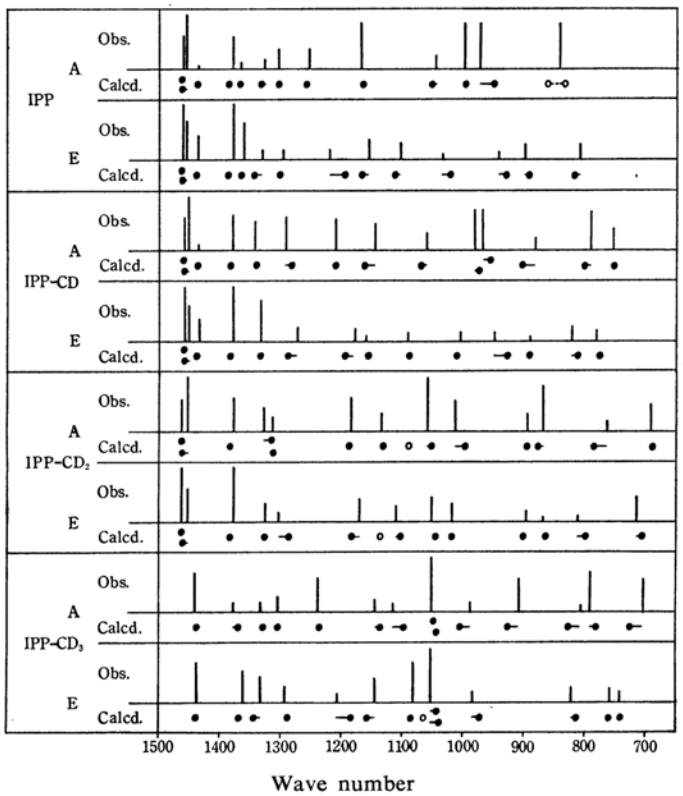

Fig. 2 Observed frequencies (cm^{-1}) and relative intensities (Ref. 7) and calculated frequencies of isotactic polypropylene [IPP], poly(propylene-2-d) [IPP-CD], poly(propylene-1, 1-d_2) [IPP-CD_2], and poly(propylene-3, 3, 3-d_3) [IPP-CD_3].

TABLE III. THE C-H AND C-D STRETCHING FREQUENCIES OF ISOTACTIC POLYPROPYLENE [IPP], POLY(PROPYLENE-2-d) [IPP-CD], POLY(PROPYLENE-1, 1-d_2) [IPP-CD_2], POLY(PROPYLENE-3, 3, 3-d_3) [IPP-CD_3]

IPP	IPP-CD	IPP-CD_2	IPP-CD_3	ν_{calcd}	Assignment
2959(vs, ∥)	2959(vs, ∥)	2961(vs, ∥)		2962(A) 2962(E)	CH_3 asym. stretch. (antisym. with respect to the H-C-CH_3 plane)
2950(vs, ⊥)	2950(vs, ⊥)	2949(vs, ⊥)		2962(E) 2962(A)	CH_3 asym. stretch. (sym. with respect to the H-C-CH_3 plane)
2921(vs, ⊥)		2922(s, ⊥)	2918(vs, ⊥)	2923～2927(E) 2924～2926(A)	CH stretch.
2879(s, ⊥)	2882(sh, ⊥)		2885(m, ⊥)	2903～2906(E) 2906(A)	CH_2 antisym. stretch.
	2868(w, ∥)	2874(m, ∥)		2873～2874(A)	CH_3 sym. stretch.
2868(s, ⊥)	2867(m, ⊥)	2868(s, ⊥)		2873～2874(E)	
2838(m)	2837(s)		2837(s)	2848～2849(E) 2845～2848(A)	CH_2 sym. stretch.
			2215(vs, ∥)	2196(A) 2196(E)	CD_3 asym. stretch. (antisym. with respect to the H-C-CD_3 plane)
			2204(s, ⊥)	2196(E) 2196(A)	CD_3 asym. stretch. (sym. with respect to the H-C-CD_3 plane)
		2171(s, ⊥) 2169(w, ∥)		2153(E) 2154(A)	CD_2 antisym. stretch.
	2162(m, ⊥) 2154(w, ∥)			2141(E) 2142(A)	CD stretch.
		2092(m, ⊥) 2085(m, ∥)		2065(E) 2062(A)	CD_2 sym. stretch.
			2067(m, ⊥) 2066(m, ∥)	2058(E) 2058(A)	CD_3 sym. stretch.

TABLE IV. THE OBSERVED AND CALCULATED FREQUENCIES (IN cm^{-1}) AND POTENTIAL ENERGY DISTRIBUTIONS (IN %) OF ISOTACTIC POLYPROPYLENE IN THE REGION 1500~600 cm^{-1}

ν_{obs}*1	ν_{calcd}	Potential energy distributions*2
1460(s, ⊥)	1463(ν_7^E)	CH_3 δ_a(ax : 10, eq : 70)
	1462(ν_7^A)	CH_3 δ_a(ax : 30, eq : 50)
1454(m, ∥)	1461(ν_8^A)	CH_3 δ_a(ax : 50, eq : 30)
	1461(ν_8^E)	CH_3 δ_a(ax : 75, eq : 10)
1435(m, ⊥)	1439(ν_9^E)	CH_2 bend. (100)
	1436(ν_9^A)	CH_2 bend. (100)
1378(m, ∥)	1385(ν_{10}^A)	CH_3 δ_s(90)
1377(s, ⊥)	1386(ν_{10}^E)	CH_3 δ_s(85)
1365(vw, ∥)	1367(ν_{11}^A)	CH_2 wag. (40), CH bend.^{ax} (30), CH_3 δ_s(15)
1360(m, ⊥)	1365(ν_{11}^E)	CH bend.^{eq} (30), CH_2 twist. (20), CH_2 wag. (15), CH_3 δ_s (15)
1330(w, ⊥)	1344(ν_{12}^E)	CH_2 wag. (35), CH bend.^{ax} (35)
1326(vw, ∥)	1332(ν_{12}^A)	CH bend.^{eq} (60)
1304(m, ∥)	1304(ν_{13}^A)	CH_2 wag. (50), CH_2 twist. (25), CH bend.^{ax} (15)
1296(w, ⊥)	1301(ν_{13}^E)	CH_2 wag. (40), CH bend. (ax : 20, eq : 20)
1254(m, ∥)	1264(ν_{14}^A)	CH_2 twist. (35), CH bend. (ax : 20, eq : 10)
1220(w, ⊥)	1195(ν_{14}^E)	CH_2 twist. (25), CH bend. (15), r_{CC}^{eq}(20)
1168(s, ∥)	1165(ν_{15}^A)	r_{CC}^{ax} (40), CH_3 rock.^{ax} (25)
1155(m, ⊥)	1166(ν_{15}^E)	r_{CM} (20). CH bend. (15)
1103(m, ⊥)	1112(ν_{16}^E)	CH_3 rock. (ax : 20, eq : 10), r_{CC}^{ax} (25)
1045(m, ∥)	1051(ν_{16}^A)	r_{CM} (35), r_{CC}^{eq} (30)
1034(vw, ⊥)	1021(ν_{17}^E)	r_{CM} (30), CH_2 twist. (15), CH bend. (15), CH_3 rock.^{eq} (15)
998(s, ∥)	996(ν_{17}^A)	CH_3 rock.^{eq} (35), r_{CM} (35), CH bend. (15), CH_2 twist. (15)
973(s, ∥)	950(ν_{18}^A)	CH_3 rock.^{ax} (50), r_{CC}^{ax} (20), r_{CC}^{eq} (20)
941(w, ⊥)	930(ν_{18}^E)	CH_3 rock. (ax : 35, eq : 10), r_{CC}^{ax} (35)
899(m, ⊥)	892(ν_{19}^E)	CH_3 rock.^{eq} (35), CH_2 rock. (20), CH bend.^{eq} (15)
842(s, ∥)	862(ν_{19}^A)	CH_3 rock. (ax : 10, eq : 25), r_{CC}^{eq} (30)
	833(ν_{20}^A)	CH_2 rock. (75), CH bend.^{ax} (15)
809(m, ⊥)	818(ν_{20}^E)	CH_2 rock. (35), r_{CM} (25), r_{CC}^{eq} (20)

*1 s, strong ; m, medium ; w, weak ; vw, very weak ; ∥, parallel band ; and ⊥, perpendicular band (observed by Peraldo and Farina[7]).

*2 CH_3 δ_s and δ_a, the symmetric and asymmetric deformation modes, respectively, of the methyl group ; r_{CM}, C-methyl stretching ; r_{CC}^{ax} and r_{CC}^{eq}, axial and equatorial C-C stretching modes, respectively.

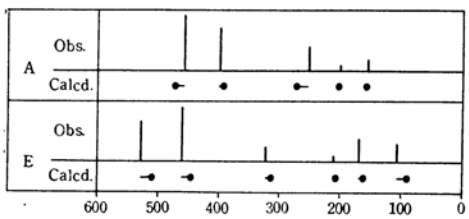

Fig. 3 Observed frequencies (cm^{-1}) and relative intensities (Refs. 1 and 8) and calculated frequencies of isotactic polypropylene (A : parallel band, E : perpendicular band) in the region below 600 cm^{-1}.

are shown in Tables IV–IX, which list only the terms greater than 15%.

The calculated frequencies of IPP below 650 cm^{-1} did not agree with the observed frequencies as closely as did the calculated higher frequencies. The potential constants, H(C-C-C), F(C-C-C), κ(CH), and Y(C-C) [CH-CH_2 bond], are primarily associated with these low frequency vibrations, accordingly, their standard errors are calulated to be relatively large. The correction terms for the Urey-Bradley force field are undoubtedly necessary for more refined treatments of the low frequency vibrations, but they have not been established as yet. The r. m. s. frequency deviation for the vibrations of IPP below 650 cm^{-1} is 3.7% except for the ν_{26}^E vibration at 106 cm^{-1}. This lowest frequency vibration is possibly considerably affected by the intermolecular force field.

C–H and C–D Stretching Vibrations

The infrared spectra of IPP and deuterated derivatives in the 3000~2000 cm^{-1} region have been measured by Peraldo and Farina,[7] by Liang et al.[11] and by McDonald and Ward.[12] Their assignments, as well as the

11) C. Y. Liang, M. R. Lytton and C. J. Boone, *J. Polymer Sci.*, **47**, 139 (1960).
12) M. P. McDonald and I. M. Ward, *Polymer (London)*, **2**, 341 (1961).

TABLE V. THE CALCULATED AND OBSERVED FREQUENCIES (IN cm^{-1}) AND POTENTIAL ENERGY DISTRIBUTIONS (IN %) OF ISOTACTIC POLY(PROPYLENE-2-d) IN THE REGION 1500~600 cm^{-1}

ν_{obs}*1	ν_{calcd}	Potential energy distributions*2
1459(s, ⊥)	1459(ν_7^E)	CH_3 δ_a (ax : 25, eq : 65)
	1459(ν_7^A)	CH_3 δ_a (ax : 20, eq : 65)
1451(s, ∥)	1460(ν_8^A)	CH_3 δ_a (ax : 65, eq : 20)
	1460(ν_8^E)	CH_3 δ_a (ax : 65, eq : 25)
1435(m, ⊥)	1438(ν_9^E)	CH_2 bend. (100)
	1436(ν_9^A)	CH_2 bend. (100)
1379(m, ∥)	1382(ν_{10}^A)	CH_3 δ_s (100)
1378(s, ⊥)	1383(ν_{10}^E)	CH_3 δ_s (100)
1342(m, ∥)	1340(ν_{11}^A)	CH_2 wag. (85)
1334(m, ⊥)	1333(ν_{11}^E)	CH_2 wag. (85)
1291(m, ∥)	1282(ν_{12}^A)	CH_2 twist. (75)
1273(w, ⊥)	1289(ν_{12}^E)	CH_2 twist. (55)
1210(m, ∥)	1210(ν_{13}^A)	r_{CC}^{ax} (25), r_{CC}^{eq} (25), CH_3 rock. (15), CD bend. (ax : 15, eq : 10)
1179(w, ⊥)	1195(ν_{13}^E)	r_{CM} (20), r_{CC}^{eq} (15), CD bend. (15), CH_3 rock. (15)
1160(vw, ⊥)	1156(ν_{14}^E)	r_{CC}^{ax} (25), CH_3 rock.^{ax} (25)
1145(m, ∥)	1162(ν_{14}^A)	CH_3 rock. (ax : 15, eq : 15), CD bend.^{eq} (15)
1091(w, ⊥)	1089(ν_{15}^E)	CH_3 rock.^{eq} (30), r_{CM} (15)
1060(w, ∥)	1070(ν_{15}^A)	CH_3 rock.^{eq} (25), CH_2 rock. (20)
1005(w, ⊥)	1010(ν_{16}^E)	CH_3 rock. (ax : 15, eq :10), CH_2 rock. (20), CD bend. (15)
981(s, ∥)	974(ν_{16}^A)	r_{CM} (40), CH_3 rock.^{ax} (25), CD bend.^{ax} (15)
969(s, ∥)	955(ν_{17}^A)	CH_3 rock. (ax : 25, eq : 15), r_{CC}^{ax} (20), r_{CM} (15)
949(w, ⊥)	927(ν_{17}^E)	r_{CC}^{ax} (40), CH_3 rock. (ax : 30, eq : 10), r_{CC}^{eq} (15)
890(vw, ⊥)	891(ν_{18}^E)	CD bend. (ax : 40, eq 10), r_{CM} (20)
881(w, ∥)	903(ν_{18}^A)	r_{CC}^{eq} (55), CD bend.^{eq} (15)
821(m, ⊥)	812(ν_{19}^E)	CD bend. (ax : 10, eq : 30), r_{CM} (20), CH_3 rock.^{eq} (15)
790(s, ∥)	801(ν_{19}^A)	CD bend.^{eq} (50), CH_3 rock. (ax : 10, eq : 20)
781(w, ⊥)	776(ν_{20}^E)	CD bend. (ax : 25, eq : 30), CH_2 rock. (35)
754(m, ∥)	752(ν_{20}^A)	CH_2 rock. (50), CD bend.^{ax} (50)

*1,*2 See *1,*2 of Table IV.

observed spectra, were critically reviewed in the present study with reference to the calculated frequencies and their possible shifts due to the anharmonicity. It was expected that the observed C–H stretching frequency would be slightly lower than the calculated C–H stretching frequency, while the observed C–D stretching frequency would be slightly higher than the calculated frequency in the final stage of the calculation based on the method of least squares.

The observed frequencies, intensities, and dichroism of IPP and deuterated derivatives,[7] the calculated frequencies, and the vibrational assignments are shown in Table III. When the potential energy distribution was calculated for each vibration, the potential energy was found to be localized in the single mode as listed in Table III.

The band at about 2870 cm^{-1} has been assigned by Liang et al.[11] to the CH_3 symmetric stretching vibration.*3 The parallel component (A) is weaker than the perpendicular component (E), in accordance with the expected intensity ratio of $I_A/I_E=0.4$.[13] The bands due to the CH_3 asymmetric stretching mode[7,11-13] are split into two components of nearly the same intensity; the parallel component at about 2960 cm^{-1} is assigned to the mode which is antisymmetric with respect to the H–C–CH_3 plane [denoted as $\nu_a(CH_3)_0$[13]]. The dichroism of this component has been estimated to be $I_E/I_A=0.1$. The perpendicular component at about 2950 cm^{-1} is assigned to the mode which is symmetric with respect to the H–C–CH_3 plane [denoted as $\nu_a(CH)_i$[13]]. The dichroism of this component has been estimated to be $I_A/I_E=0.8$. The stretching vibrations of the CD_3 groups are observed at 2215 cm^{-1} (∥) and 2204 cm^{-1} (⊥) [asymmetric] and at 2066~2067 cm^{-1} [symmetric].

The nondichroic band at 2838 cm^{-1} has been assigned to the CH_2 symmetric stretching mode.[7,11-13] The perpendicular band at about 2880 cm^{-1} is assigned, in the present study, to the CH_2 antisymmetric stretching vibration.*4

*3 Krimm assigned this band to an overtone,[13] whereas McDonald and Ward[12] assigned the two bands at 2925 and at 2868 cm^{-1} to the CH_3 symmetric stretching modes.

13) S. Krimm, *Fortschr. Hochpolymer.-Forsch.*, **2**, 51 (1960).

*4 This band has been assigned to the CH_3 symmetric stretching mode (E) [13] or to an overtone.[11,12]

TABLE VI. THE OBSERVED AND CALCULATED FREQUENCIES (IN cm^{-1}) AND POTENTIAL ENERGY DISTRIBUTIONS (IN %) OF ISOTACTIC POLY(PROPYLENE-1, 1-d_2) IN THE REGION 1500~600 cm^{-1}

ν_{obs}*1	ν_{calcd}	Potential energy distributions*2
1461(s, ⊥)	1462(ν_7^E)	CH_3 δ_a (ax : 20, eq : 60)
	1462(ν_7^A)	CH_3 δ_a (ax : 20, eq : 60)
1452(s, ∥)	1461(ν_8^A)	CH_3 δ_a (ax : 65, eq : 20)
	1460(ν_8^E)	CH_3 δ_a (ax : 65, eq : 20)
1377(s, ⊥)	1383(ν_9^E)	CH_3 δ_s (100)
	1383(ν_9^A)	CH_3 δ_s (100)
1327(m, ∥)	1315(ν_{10}^A)	CH bend. (ax : 10, eq : 65)
1325(m, ⊥)	1326(ν_{10}^E)	CH bend. (ax : 15, eq : 55)
1313(w, ∥)	1312(ν_{11}^A)	CH bend. (ax : 65, eq : 10)
1303(w, ⊥)	1286(ν_{11}^E)	CH bend. (ax : 65, eq : 15)
1184(s, ∥)	1187(ν_{12}^A)	r_{CC}^{ax} (45), CD_2 wag. (20)
1170(m, ⊥)	1183(ν_{12}^E)	r_{CC}^{eq} (35)
	1136(ν_{13}^E)	r_{CC}^{ax} (30), CD_2 wag. (20), r_{CM} (15), CH_3 rock. (15)
1134(m, ∥)	1131(ν_{13}^A)	CH_3 rock.^{eq} (15), CD_2 twist. (15), r_{CM} (15)
1110(m, ⊥)	1102(ν_{14}^E)	CH_3 rock.^{eq} (25), CD_2 wag. (15)
	1088(ν_{14}^A)	r_{CM} (20), r_{CC}^{eq} (20), CH_3 rock.^{ax} (20)
1058(s, ∥)	1052(ν_{15}^A)	CD_2 bend. (60), CH_3 rock.^{eq} (15)
1051(m, ⊥)	1045(ν_{15}^E)	CD_2 bend. (75)
1018(m, ⊥)	1018(ν_{16}^E)	CD_2 wag. (40), CH_3 rock.^{ax} (25), r_{CM} (20)
1013(s, ∥)	996(ν_{16}^A)	r_{CM} (30), CD_2 wag. (20), r_{CC}^{eq} (20), CH_3 rock.^{ax} (20)
896(w, ⊥)	901(ν_{17}^E)	CH_3 rock. (ax : 10, eq : 25), r_{CC}^{ax} (20)
894(m, ∥)	895(ν_{17}^A)	CH_3 rock.^{eq} (25), CD_2 wag. (20), CD_2 twist. (25)
868(s, ∥)	877(ν_{18}^A)	CH_3 rock. (ax : 30, eq : 20), CH bend. (15), r_{CC}^{ax} (15)
868(w, ⊥)	865(ν_{18}^E)	CH_3 rock. (ax : 20, eq : 15), r_{CC}^{ax} (20), CD_2 twist. (20)
811(w, ⊥)	799(ν_{19}^E)	CD_2 twist. (55)
764(w, ∥)	785(ν_{19}^A)	CD_2 twist. (40), r_{CC}^{eq} (20), r_{CM} (15)
715(m, ⊥)	705(ν_{20}^E)	CD_2 rock. (50), r_{CM} (15)
691(m, ∥)	689(ν_{20}^A)	CD_2 rock. (80)

*1,*2 See *1,*2 of Table IV.

The corresponding bands of the CD_2 group are observed at about 2170 cm^{-1} (antisymmetric stretching), while the bands due to the CD_2 symmetric stretching mode[7] appear to be split into the parallel component at 2085 cm^{-1} and the perpendicular component at 2092 cm^{-1}. The stretching vibrations of the CHD group of poly(propylene-1-d_1) are observed at 2870 cm^{-1} (CH stretching) and at about 2135 cm^{-1} (CD stretching).[7,14]

The strong perpendicular bands at about 2920 cm^{-1} are assigned to the stretching vibration of tertiary CH group in the present study.*5 The perpendicular component has been expected to be stronger than the parallel component ($I_A/I_E=0.8$).[13] The band due to the CD stretching vibration[7] appears to be split into the weak parallel component at 2154 cm^{-1} and the strong perpendicular component at 2162 cm^{-1}.

*5 This band has been assigned to the CH_2 antisymmetric stretching mode.[11-13] Instead, the bands near 2800 cm^{-1} have been assigned to the CH stretching modes.[12,13]

14) T. Miyazawa and Y. Ideguchi, to be published.

Infrared Bands in the 1500~650 cm^{-1} Region

In our previos study, the potential energy distributions for the vibrations lying in the 1500~650 cm^{-1} region have been approximately calculated and the vibrational assignments of the infrared bands discussed in detail.[2] In the present study, the potential energy distributions (PED) were refined by a complete normal coordinate treatment (Table IV–VII). However, the potential energy distributions did not change essentially, except as noted below: (1) The potential energy of the vibrations of IPP at 1377~1379 cm^{-1} are associated almost exclusively with the CH_3 symmetric deformation mode, although in the previous treatment a slight coupling with the C–H bending modes was deduced. (2) As for the C–H and C–D bending modes, and the degenerate deformation and rocking modes of the CH_3 and CD_3 groups, the fractions of the potential energy associated with the axial and equatorial components have changed more or less for several vibrations. Except for these changes, the detailed analyses of the infrared bands reported previously are still valid. Therefore,

TABLE VII. THE OBSERVED AND CALCULATED FREQUENCIES (IN cm^{-1}) AND POTENTIAL ENERGY DISTRIBUTIONS (IN %) OF ISOTACTIC POLY(PROPYLENE-3, 3, 3-d_3) IN THE REGION 1500～600 cm^{-1}

ν_{obs}*1	ν_{calcd}	Potential energy distributions*2
1440(m, ∥)	1437(ν_7^A)	CH_2 bend. (100)
1438(m, ⊥)	1439(ν_7^E)	CH_2 bend. (100)
1379(w, ∥)	1369(ν_8^A)	CH_2 wag. (45), CH bend.^{ax} (35)
1361(m, ⊥)	1367(ν_8^E)	CH bend.^{eq} (35), CH_2 wag. (20), CH_2 twist. (25)
1334(w, ∥)	1329(ν_9^A)	CH bend.^{eq} (60), CH_2 twist. (15)
1333(m, ⊥)	1343(ν_9^E)	CH_2 wag. (40), CH bend.^{ax} (35)
1305(m, ∥)	1305(ν_{10}^A)	CH_2 wag. (50), CH_2 twist. (25), CH bend.^{ax} (20)
1293(m, ⊥)	1288(ν_{10}^E)	CH bend. (ax : 30, eq : 25), CH_2 wag. (35)
1239(m, ∥)	1236(ν_{11}^A)	CH bend. (ax : 25, eq : 25), CH_2 twist. (35)
1206(w, ⊥)	1183(ν_{11}^E)	CH_2 twist. (25), CH bend. (ax : 15, eq : 10), r_{CC}^{eq} (20)
1145(m, ⊥)	1156(ν_{12}^E)	r_{CM} (30), CH bend. (20)
1145(w, ∥)	1136(ν_{12}^A)	r_{CC}^{ax} (55)
1115(w, ∥)	1097(ν_{13}^A)	CD_3 δ_s (70), r_{CM} (45)
1081(m, ⊥)	1085(ν_{13}^E)	CD_3 δ_s (35), r_{CC}^{ax} (25), r_{CC}^{eq} (15)
	1064(ν_{14}^E)	CD_3 δ_s (35), CD_3 δ_a^{ax} (15), r_{CC}^{ax} (20)
1054(s, ⊥)	1043(ν_{15}^E)	CD_3 δ_a (ax : 15, eq : 80)
	1048(ν_{14}^A)	CD_3 δ_a (ax : 15, eq : 65)
1051(s, ∥)	1043(ν_{15}^A)	CD_3 δ_a (ax : 75, eq : 15)
	1038(ν_{16}^E)	CD_3 δ_a (ax : 60, eq : 10)
989(w, ∥)	1005(ν_{16}^A)	r_{CC}^{eq} (40), CD_3 δ_s (20)
984(w, ⊥)	971(ν_{17}^E)	CH_2 rock. (15), r_{CM} (15), CD_3 δ_s (15)
909(m, ∥)	926(ν_{17}^A)	r_{CM} (25)
821(m, ⊥)	814(ν_{18}^E)	CH_2 rock. (30), r_{CM} (15)
807(vw, ∥)	827(ν_{18}^A)	CH_2 rock. (70), CH bend. (15)
791(s, ∥)	781(ν_{19}^A)	CD_3 rock. (ax : 40, eq : 35)
759(m, ⊥)	760(ν_{19}^E)	CD_3 rock. (ax : 50, eq : 20)
743(w, ⊥)	741(ν_{20}^E)	CD_3 rock. (ax : 15, eq : 50)
703(m, ∥)	725(ν_{20}^A)	CD_3 rock. (ax : 40, eq : 35)

*1,*2 See *1,*2 of Table IV.

TABLE VIII. THE FREQUENCIES (IN cm^{-1}) OF THE FAR INFRARED BANDS AND THE POTENTIAL ENERGY DISTRIBUTIONS (%) OF ISOTACTIC POLYPROPYLENE

ν_{obs}*1	ν_{calcd}*2	Potential energy distributions*3
528(⊥)	ν_{21}^E 509	δ^a (40), δ (25)
460(⊥)	ν_{22}^E 445	δ^s (65)
456(∥)	ν_{21}^A 473	δ^a (75)
398(∥)	ν_{22}^A 392	δ^s (35), δ^a (40)
321(⊥)	ν_{23}^E 314	δ^a (60)
251(∥)	ν_{23}^A 272	δ^s (40), δ^a (20)
210(⊥)	ν_{24}^E 207	t_{C-CH_3} (95)
200(∥)	ν_{24}^A 203	t_{C-CH_3} (85)
169(⊥)	ν_{25}^E 162	δ^a (40), δ (30), t_{CC}^{ax} (15)
155(∥)	ν_{25}^A 157	δ (40), t_{CC}^{eq} (35)
106	ν_{26}^E 90	t_{CC}^{ax} (70)

*1 Observed frequencies (Refs. 1 and 8); ∥ : parallel band; and ⊥ : perpendicular band.
*2 Calculated frequencies.
*3 δ^s and δ^a : the symmetric and asymmetric deformation modes of the C-CH-C group (CH carbon bonded to C); δ : C-CH_2-C bending; t_{CC}^{eq}, t_{CC}^{ax} and t_{C-CH_3} : the internal rotation modes about the equatorial and axial C-C bonds and the C-methyl bond, respectively.

TABLE IX. FREQUENCIES (ν_c IN cm^{-1}) AND POTENTIAL ENERGY DISTRIBUTIONS (PED IN %)*1 CALCULATED FOR THE LOW FREQUENCY VIBRATIONS

$[-CH_2-CD(CH_3)-]_\infty$

A species		E species	
ν_c	PED	ν_c	PED
467	δ^a (75)	497	δ^a (35), δ (25)
387	δ^s (35), δ^a (40)	438	δ^s (65)
269	δ^s (40), δ^a (20)	310	δ^a (60)
202	t_{C-CH_3} (85)	207	t_{C-CH_3} (95)
154	t_{CC}^{eq} (35), δ (35)	160	δ^a (40), δ (30), t_{CC}^{ax} (15)
		89	t_{CC}^{ax} (75)

$[-CD_2-CH(CH_3)-]_p$

A species		E species	
ν_c	PED	ν_c	PED
446	δ^a (70)	483	δ^a (40), δ (30)
367	δ^s (40), δ^a (30)	394	δ^s (60), CD_2 rock. (15)
249	δ^s (30), δ^a (25), t_{C-CH_3} (15)	297	δ^a (60)
202	t_{C-CH_3} (80)	207	t_{C-CH_3} (95)
153	t_{CC}^{eq} (35), δ (35)	155	δ^a (40), δ (30), t_{CC}^{ax} (15)
		88	t_{CC}^{ax} (70)

$[-CH_2-CH(CD_3)-]_p$

A species		E species	
ν_c	PED	ν_c	PED
441	δ^a (65)	484	δ^a (30), δ (25)
362	δ^s (30), δ^a (45)	420	δ^s (60)
260	δ^s (40), δ^a (20), t_{CC}^{eq} (15)	291	δ^a (60)
154	t_{C-CD_3} (50), δ (20)	157	t_{C-CD_3} (45), δ^a (25), δ (15)
137	t_{C-CD_3} (40), t_{CC}^{eq} (25), δ (20)	138	t_{C-CD_3} (55), δ^a (20), δ (15)
		82	t_{CC}^{ax} (75)

*1 See *3 of Table VIII.

the nature of the infrared bands of IPP, IPP-CD, IPP-CD_2 and IPP-CD_3 will be briefly described.

$[-CH_2CH(CH_3)-]_p$.—The perpendicular band at 1460 cm^{-1} and the parallel band at 1454 cm^{-1} are assigned to the CH_3 asymmetric deformation vibrations, while the bands at 1377~1378 cm^{-1} are assigned to the CH_3 symmetric deformation vibrations. The bands of IPP, IPP-CD, and IPP-CD_3 at 1435~1440 cm^{-1} are assigned to the CH_2 bending vibrations. The abnormal dichroic behavior of the bands of IPP and IPP-CD may possibly be due to the slight coupling of the CH_2 and CH_3 deformation modes.[2]

In the 1370~1200 cm^{-1} region, the observed bands are due to the hybridized vibrations of the CH_2 wagging and twisting modes and the axial and equatorial CH bending modes.*6 The interactions among these modes are primarily due to the trans- and gauche-coupling terms in the vibrational potential function. These vibrational couplings depend upon the internal-rotation about the main-chain CH–CH_2 bonds. The remarkable spectral change upon the fusion of the isotactic sample may be understood in relation to the coupling of the CH_2 and CH modes across the CH–CH_2 bonds.

The infrared bands of IPP in the 1200~800 cm^{-1} region arise from the hybridized vibrations of the axial and equatorial C–C stretching modes, the C–methyl stretching modes, the axial and equatorial CH_3 rocking modes, and the CH_2 rocking modes. The strong parallel bands at 1168, 998, and 973 cm^{-1} are primarily due to the C–C stretching and CH_3 rocking modes. The parallel bands at 973 cm^{-1} and 1168 cm^{-1} arise from the coupled vibrations of the antisymmetric stretching mode of the axial and equatorial C–C bonds and of the methyl rocking modes, which is nearly antisymmetric with respect to the H–C–CH_3 plane. For the 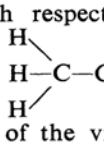 group, the atomic displacements of the vibrations at 973 cm^{-1} and 1168 cm^{-1} are schematically

*6 The intrinsic frequencies of the CH_2 wagging and twisting modes are located at 1330~1340 cm^{-1} and 1270~1290 cm^{-1} respectively, while the intrinsic C-H bending frequency is located at 1305~1325 cm^{-1}.

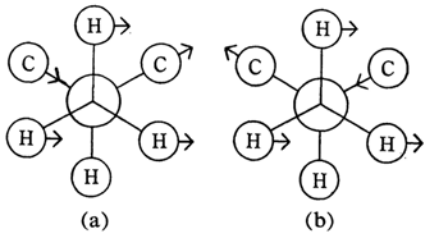

Fig. 4 Atomic displacements of the vibrations of $H-\overset{H}{\underset{H}{C}}-\overset{C}{\underset{C}{C}}-H$ group at 950 cm^{-1} (a) and at 1150 cm^{-1} (b).

shown in Figs. 4a and 4b respectively. The band at 998 cm^{-1} arises from the C-methyl stretching mode and the methyl rocking mode in the H-C-CH_3 plane. The parallel band at 842 cm^{-1} is due either to the ν_{19}^A vibration or to the ν_{20}^A vibration. The ν_{19}^A vibration is associated with the methyl rocking mode (in the H-C-CH_3 plane) as coupled with the nearly symmetric stretching mode of the axial and equatorial C-C bonds and the C-methyl bonds.

[-CH_2-$CD(CH)_3$-]$_p$—Since the intrinsic C-D bending frequency is much lower than 1250 cm^{-1}, the CH_2 wagging and twisting modes of this molecule are not coupled with the C-D bending modes. The bands at 1342 cm^{-1} ($\parallel$) and 1334 cm^{-1} ($\perp$) are due to the CH_2 wagging modes, while the bands at 1291 cm^{-1} ($\parallel$) and 1273 cm^{-1} ($\perp$) are due to the CH_2 twisting modes. The infared bands of IPP-CD in the 1250~750 cm^{-1} region arise from the coupled vibrations of the C-D bending modes, the CH_3 and CH_2 rocking modes, and the C-C stretching modes. The intrinsic frequencies of all these modes may be located in the 1100~800 cm^{-1} region. It is remarkable to note that the contributions of the C-D bending modes are greater than 15% for many vibrations in the 1250~750 cm^{-1} region.

[-CD_2-$CH(CH_3)$-]$_p$.—For this molecule, the intrinsic CD_2 wagging and twisting frequencies are shifted lower than 1200^{-1}, and, consequently, the CH bending modes are not coupled with the CD_2 bending modes. The bands at 1327 cm^{-1}, 1325 cm^{-1}, 1313 cm^{-1}, and 1303 cm^{-1} arise almost exclusively from the C-H bending modes.

The bands primarily due to the CD_2 bending modes are observed at 1058 cm^{-1} ($\parallel$) and 1051 cm^{-1} ($\perp$), while the band due to the CD_2 rocking modes are observed at 764 cm^{-1} ($\parallel$) and 811 cm^{-1} ($\perp$).

The CD_2 wagging and twisting modes are strongly coupled with the methyl rocking modes and the C-C stretching modes and give rise to the infrared bands in the 1200~800 cm^{-1} region.

[-CH_2-$CH(CD_3)$-]$_p$.—The strong bands of IPP-CD_3 at 1051 cm^{-1} ($\parallel$) and at 1054 cm^{-1} ($\perp$) are due to the CD_3 asymmetric deformation modes. The CD_3 symmetric deformation modes are strongly coupled with the axial and equatorial C-C stretching modes and give rise to bands in the 1100~1000 cm^{-1} region. The parallel bands at 791 and 703 cm^{-1} and the perpendicular bands at 759 and 743 cm^{-1} arise from the CD_3 rocking modes.

Far Infrared Vibrations of Isotactic Polypropylene

The far infrared spectra of the uniaxially oriented films of isotactic polypropylene have been measured in the 600~300 cm^{-1} region[1] and in the 400~80 cm^{-1} region[8] (the dichroism has been measured in the region above 100 cm^{-1}). (A preliminary normal coordinate treatment had previously been made as an aid in the vibrational assignments.[8]) The potential energy distributions of the far infrared vibrations of isotactic polypropylene were recalculated in the present study and are listed in Table VIII.

These low frequency vibrations are associated with the C-C-C bending modes of the $C-CH_2-C$ and $C-CH\langle^{C}_{C}$ groups and with the internal-rotation modes about the C-methyl bond and the equatorial and axial C-C bonds. The weak bands at 200 cm^{-1} ($\parallel$) and 210 cm^{-1} ($\perp$) arise from the internal-rotation modes of the CH_3 group about the C-methyl bond. The low frequency modes of isotactic polypropylene are not localized in a repeating unit. Therefore, these modes give rise to well-defined bands only for highly-ordered helical conformations in the crystalline region.[8]

The far infrared spectra of the deuterated derivatives of isotactic polypropylene have not been published. However, the frequencies and potential energy distributions calculated for deuterated derivatives are shown in Table IX.

Liquid Spectra of Isotactic Polypropylene

Well-defined infrared bands observed in the liquid spectra of isotactic polypropylene and deuterated derivatives have been discussed before with reference to the potential energy distributions calculated for the helical structure. Moreover, the liquid bands arising from the CH_3 symmetric and asymmetric deformation modes, the CH_2 bending wagging, and twisting modes and the CH bending modes,

and the CD_3 rocking modes have already been analyzed.[2)]

For isotactic polypropylene, two strong bands are observed at 971 and 1151 cm^{-1} in the liquid state; these are naturally considered to arise from the C–C stretching modes and the methyl rocking modes. An empirical analysis has been made before in view of the "intrinsic" methyl rocking frequency.[2)] In the present study, the normal vibrations of the model

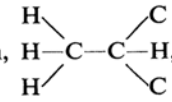

system, H–C(H)(C)–C(H)(C)–H, were treated. The elements of the potential energy matrix were transferred from the corresponding elements of isotactic polypropylene. In the 1200~800 cm^{-1} region, three A′ vibrations (symmetric with respect to the H–C–CH_3 plane) were calculated at 864, 1015 and 1062 cm^{-1}, whereas two A″ vibrations (antisymmetric with respect to the H–C–CH_3 plane) were calculated at 948 cm^{-1} (ν_a) and 1134 cm^{-1} (ν_b). The atomic displacements of the ν_a and ν_b vibrations are schematically shown in Fig. 4. The calculated vibration at 948 cm^{-1} appears to correspond to the liquid frequency of 971 cm^{-1}, and its potential energy is associated 60% with the rocking mode and 40% with the C–C stretching modes. On the other hand, the calculated vibration at 1134 cm^{-1} corresponds to the liquid frequency of 1151 cm^{-1}, and its potential energy is associated 50% with the C–C stretching mode and 20% with the methyl rocking mode. If either one of these vibrations is excited in phase throughout the main chain, as is shown in Fig. 5, the vibrations of adjacent units will

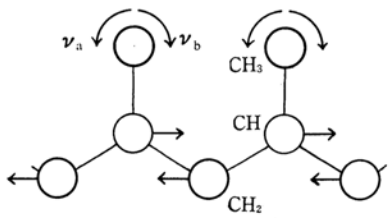

Fig. 5. In-phase vibrations of the ν_a or ν_b mode.

tend to displace the common CH_2 group in nearly the same direction (at least not in the opposite direction), and only minor vibrational interactions may be expected among CH–CH_3 groups. Such a vibrational mode may not be very sensitive to changes in the internal-rotation arrangements, and accordingly, well-defined strong absorption peaks may be expected, even in the liquid state. In support of these considerations, the in-phase ν_a and ν_b vibrations give rise to the strong bands at 973 cm^{-1} and 1168 cm^{-1} for isotactic polypropylene (in the crystalline region) and to the strong bands at 1153 cm^{-1} and 974 cm^{-1} for syndiotactic polypropylene (in the crystalline region).[15)]

The strong parallel band of isotactic polypropylene at 998 cm^{-1} disappears on melting. As Table IV shows, this band is due to the hybridized vibration of the methyl rocking mode, the C–methyl stretching mode, and the CH_2 twisting mode. The coupling with the CH_2 twisting mode depends upon the internal-rotation about the main-chain CH–CH_2 bonds. This vibration, therefore, is very much affected by the rearrangements of the main-chain conformations and does not give rise to a well-defined band in the liquid state.

Summary

The infrared active normal vibrations of isotactic polypropylene and its deuterated derivatives in the crystalline state have been treated. The modified Urey-Bradley-Shimanouchi force field has been used for the calculations. A total of 23 potential constants have been adjusted by the method of least squares with reference to a total of 166 frequencies observed by Peraldo and Farina. The standard errors of the potential constants have also been calculated. The r. m. s. deviation of the calculated frequencies from the observed ones is as small as 0.9%. The potential energy distributions have also been calculated for the discussion of the nature of the observed infrared bands. Vibrational assignments of the liquid bands of isotactic polypropylene have also been made.

The authors wish to thank Professor Takehiko Shimanouchi and his group at the University of Tokyo for their stimulating discussions and Mr. Hiroatsu Matsuura of Osaka University for his assistance in the preparation of all the figures.

Institute for Protein Research
Osaka University
Kita-ku, Osaka

15) T. Miyazawa and Y. Ideguchi, presented at the 17th Annual Meeting of the Chemical Society of Japan, Tokyo, April, 1964; T. Miyazawa, *J. Polymer Sci.*, to be published.